A continuous method for arsenic removal from groundwater using hybrid biopolymer-iron-nanoaggregates: improvement through factorial designs

Marianela Batistelli[2], Bárbara Pérez Mora[1], Florencia Mangiameli[1,2], Nadia Mamana[3], Gerardo Lopez[4], María F. Goddio[4], Sebastián Bellú *[1,2] and Juan C. González*[1,2]

[1]Área Química General e Inorgánica, Departamento de Química-Física, Facultad de Ciencias Bioquímicas y Farmacéuticas, Universidad Nacional de Rosario, Suipacha 531, S2002LRK Rosario, Santa Fe, Argentina

[2]Instituto de Química de Rosario-CONICET (IQUIR), Suipacha 570, S2002LRK Rosario, Santa Fe, Argentina

[3] Laboratorio de Materiales Cerámicos IFIR, CONICET, FCEIA, UNR, Bv. 27 de Febrero 210 Bis, 2000 Rosario, Argentina.

[4]NANOTEK SA, Parque Tecnológico Litoral Centro - Ruta Nacional 168, Argentina.

∗Corresponding author: Universidad Nacional de Rosario, Facultad de Ciencias Bioquímicas y Farmacéuticas, Suipacha 531, S2002LRK Rosario, Santa Fe, Argentina. Tel.: +54 341 4350214; e-mail addresses: gonzalez@iquir-conicet.gov.ar (Juan C. González); bellu@iquir-conicet.gov.ar (Sebastián Bellú)

Abstract

This article has been accepted for publication and undergone full peer review but has not been through the copyediting, typesetting, pagination and proofreading process which may lead to differences between this version and the Version of Record. Please cite this article as doi: 10.1002/jctb.6600

Background: Due to a variety of toxicological problems, the presence of As(V) in aquifers is a significant problem. Sorption using chitosan doped with iron nanoaggregates results in green and cheap methodology for its elimination.

Results: The hybrid sorbent was characterized by SEM, EDS, TGA, XRD, and FTIR spectroscopy. Its stability against pH and time was determined by ICP-MS, while conventional analytical techniques verified its Fe content. The sum of an individual As(V) removal capacity by chitosan and iron nanoaggregates, was smaller than that of the hybrid sorbent, indicating the existence of synergy.

Conclusion: This study demonstrates the great capacity of the hybrid sorbent to eliminate As(V) working with a continuous system (columns). The additional use of a factorial design allows determining optimal operating values to optimize two responses. In other words, in this multi-response system, column service time (tb) was minimized and, at the same time, maximized the volumes of purified water obtained ([As(V)] <0.05 m L^{-1}) using desirability function.

Keywords: ARSENIC; IRON-NANOPARTICLE; GROUNDWATER; IMPROVEMENT

1. Introduction

Arsenic (As) in water represents a global problem, affecting low- and high-income countries[1]. More than 226 million people are exposed[2] through the ingestion of contaminated drinking water and food[3]. Compounds containing As can be found in

soils, rocks and natural waters[4]. Both organic and inorganic forms are naturally found, being the last the most toxic[5]. In natural waters, it is present with two predominant oxidation states, As(III) and As(V)[6].

Argentina is one of the most affected countries in Latin America[7]. In the Chaco-Pampean plain areas, As concentrations vary in a wide range (0.005 - 5 mg L^{-1})[8]. About 50% of the population in rural areas is exposed to As poisoning, including several clinical manifestations such as cancer, hypertension, diabetes, and hyperpigmentation[9]. About 30% of the people exposed to As develop cancer, especially of skin and internal organs[10].

The guideline value of As in drinking water is 0.01 mg/L recommended by the World Health Organization[11], whereas the value of 0,05 mg/L, is valid for the Argentine drinking water standards[12].

For this reason, it is essential to develop a simple, economical, and sustainable As removal technology. Most of the current methods to remove As include oxidation/reduction, coagulation, precipitation, sorption, ionic exchange, membrane technologies, and bioremediation[13]. However, some of these methods are expensive and/or unfriendly to the environment. Biosorption is a novel method that has demonstrated a high capacity to remove several contaminants[14-17], mainly when applied in continuous flow systems[16,18]. Our previous work showed chitosan capacity to remove As from water and groundwater[16,19]. Chitosan doped with iron derived nanoparticles can increase the adsorption properties of the material. This has been reported previously in the literature[20-22]. Nanoparticles have high removal capacity and fast reaction kinetics

against contaminants due to their high surface/volume ratio. A combination of iron nanoparticles and biopolymers increase the system stability, creating a synergy for As removal[23]. The aim of this work was the synthesis of a new material based on chitosan and iron derived nanopartiples (CIN) and its use in continuous treatment of natural contaminated groundwater. The use of a factorial design allowed the determination of the operating values to optimize two responses at the same time: minimum columns service time (tb) and maximum purified water volume (Vol).

2. Experimental

2.1 Analytical methods

Groundwater natural samples were obtained from Piamonte Town, Santa Fe, Argentina. Groundwater characterization was analized by standard methods and the results are showed in **Table S1**. Water samples were supplemented by the addition of sodium arsenate ($Na_2HAsO{\cdot}7H_2O$) solution until 1.0 mg/L As(V). Arsenic concentration was increased until 1.0 mg/L in column experiments in order to work with a value within the concentration range found in natural groundwater of the area under study. All the reagents for the current research were of analytical grade. As(V) quantification in aqueous solutions was performed applying a self-made modification of molybdenum blue method[16]. Detection Limit (DL) and Quantification Limit (QL) were 0.0043 mg L^{-1} and 0.013 mg L^{-1}, respectively. The molar extinction coefficient (ε) obtained in the experimental linear range (0.0050-0.50 mg L^{-1}) was (19150 ± 150) M^{-1} cm^{-1}.

2.2 Chitosan Iron Nanoaggegates synthesis (CIN)

Iron nanoparticles synthesis and stabilization was achieved from a stock solution containing 1:2 molar ratio ferrous: ferric species, which was slowly poured (drop-wise) into an alkali source, composed of sodium hydroxide, under vigorous stirring and nitrogen sparging. Core-shell magnetic crystals (Fe^o core - magnetite and / or maghemite shell) formed and precipitated. CIN was prepared by mixing a water-based suspension of iron nanoaggregates, functionalized with starch to promote interaction and linking to chitosan, incorporated as a powder. The mixture (1:20 w/w iron/chitosan) was stirred to achieve homogenization. Then it was allowed to settle, supernatant water was eliminated, and the material was dried at 60 °C for 72 hours. The resultant solid was then ground to obtain a suitable powder.

Chitosan used for the CIN's synthesis was previously characterized (molecular weight and deacetylation degree) by our group[15,19].

2.3 CIN stability and total iron quantification

CIN stability was determined as follow: 1.0 g of CIN were mixed with 60.0 mL of acid solution (pH 4.5 given by H_2SO_4) and stirred at 350 rpm for 4.5 h. The filtered supernatant was analyzed to measure the presence of iron using ICP-MS. Quantification of total iron was carried out by disaggregation of samples, and iron in aquous phase were measured by ICP-MS.

2.4 pH zero-point charge (pH_{ZPC}) determination

Experiments were carried out preparing 50.0 mL of 0.01 M $NaNO_3$ solutions at different initial pH values, pH_0 (5.0 - 8.0). After that, 1.0 g of CIN was added to each solution and stirring for 24 hours at room temperature (25°C). The final pH (pH_f) was measured and the ΔpH was calculated. The intersection point on the x-axis in the ΔpH vs pH_0 graph indicates the pH_{ZPC}[14].

2.5 Sorbent composition effect on the As(V) sorption

Batch experiments were carried out using chitosan, iron nanoaggregates, and CIN individually. Reaction conditions like pH (4.5), T (21 ºC), initial concentration of As(V) (20 mg L^{-1}), and contact time (5.0 h), were the same. Arsenic concentration was raised up to 20 mg/L in order to magnified differences between the three materials.

Groundwater was divided into three equal parts, and each one was placed in a beaker with constant stirring. Each aliquot was mixed with different sorbents masses, calculated in proportion to the content of iron and chitosan (5.8% w/w Fe). At the end of the reaction time, solutions were filtered under reduced pressure using cellulose nitrate filters (0.45 µm pore size). Afterward, the remaining As(V) concentration was determined.

2.6 FT-IR, XRD and TGA

FT-IR spectroscopy (Perkin Elmer FT-IR Spectrum One spectrophotometer) was performed to identify the chemical functional groups present on CIN. The full

absorbance spectra in the IR wavenumber range from 500 to 4000 cm^{-1} were obtained by the KBr dilution method (1.5% w/w).

XRD measurements were carried out to evaluate the crystallinity degree of CIN, before and after As(V) treatment, on a PANalytical EMPYREAN SERIES X-ray diffractometer equipped with a graphite monochromator and CuKα radiation (1.540598 Å), a current of 30 mA and voltage of 40 kV.

TGA was performed in Thermogravimetric equipment DTG-60H, Shimadzu, made in Japan. N/P 346-68700-93, atmosphere: air, flow rate: 50 mL min-1, temperature range 30 - 650 ºC, temperature rate: 10 ºC min-1, CIN mass: 15.124 mg, CIN-As mass: 14.841 mg.

2.7 SEM and EDAX

Iron nanoaggregates size and morphology were analyzed in a Zeiss Supra 40VP field-emission scanning electron microscope (SEM). A SEM Philips 515 with EDS probe focused on individual agglomerates was used to assess the composition of nanoparticles.

2.8 Continuous Up-Flow Fixed-Bed Column Sorption Experiments

Polypropylene columns of 2.0 cm internal diameter and 9.5 cm long were used for sorption experiments. CIN sorbent was hydrated in 100 mL of Milli-Q water (pH 4.5) at room temperature with constant agitation. Hydrated sorbent was packed inside the column, reaching the desired height and packing density. Groundwater containing 1.0 mg L^{-1} of As(V) was pumped through the bed column with a peristaltic pump (Gilson

Minipuls 3) in an up-flow mode at room temperature (25°C). Volumetric flow-rate and pH were periodically controlled. Samples were eluted and collected at different times until the output As(V) concentration was equal to the input. As(V) sorption capacity (q_t) was determined from **Eq. 1**:

$$q_t = \frac{m_{in} - m_{out}}{m_s} = \frac{C_0\, Q t_e - Q \int_0^t C_{eff}(t)\, dt}{m_s} \qquad \textbf{Eq.1}$$

In Eq. **1**, q_t represent the amount of As(V) uptake per unit mass of CIN (mg g^{-1}), m_{in} and m_{out} are a total mass of As(V) input and output from the fixed-bed column (mg), m_s is the dry mass of CIN, C_0 and C_{eff} are initial and effluent As(V) concentrations (mg L^{-1}), Q is the volumetric flow-rate (L min^{-1}), t_e (min) is the column saturation time when C/C_0 = 0.95 and $Q\int_0^t C_{eff}(t)dt$ represents the elution profile area (mg). Integration limits, 0 and t, are related to 0 and 0.95 C/C_0 ratios.

Finally, As(V) removal percentage (%R) can be obtained from min and mout, through **Eq. 2**:

$$\%R = \frac{m_{in} - m_{out}}{m_{in}} \times 100 \qquad \textbf{Eq. 2}$$

Desorption studies was performed employing 0.10 M solution of NaOH eluent and an upward flow of 8.5 mL min^{-1}. The adsorption‑desorption cycles were repeated three times. Adsorption conditions: H = 2.20 cm, flow rate = 8.53 mL / min, $[As(V)]_0$ = 1.0 mg/L.

Desorption efficiency was calculated using **Eq. 3**.

$$Desorption\ efficiency\ (\%) = \frac{mol\ As\ released}{mol\ As\ adsorbed} x100 \qquad \textbf{Eq. 3}.$$

2.9 Statistical, mathematical modeling of experimental column data

Different mathematical models are used to describe the sorption process behavior. Their use allows analyzing and explaining the experimental data and predicting changes due to different operational conditions. These models include Thomas[23], Yoon−Nelson[24], and Modified Dose Response[25].

Response surface methodology (RSM) is defined as a set of mathematical and statistical techniques used to model and analyze the response of interest, which can be influenced by several variables. After preliminary tests, a central composite design (CCD) was selected for As(V) removal improvement. Design Expert (version 7.0) was used for data analysis.

Table I presents the range and levels of independent variables: volumetric flow-rate (Q) and column bed height (H).

Insert Table I here

For RSM, experimental conditions were: pH = 4.5, packing density = 270 kg / m^3, $[As(V)]_0$ = 1.0 mg / L. Evaluated factors were: H and Q.

The study of the adjustment of experimental data to the mathematical model was carried out through Analysis of the Variance (ANOVA). Being a multi-response design, where the responses selected were the t_b (the time when C/C_0 ratio is equal to 0.05) and Vol (the volume of purified water at $C/C_0 = 0.05$), the desirability function was used to find the best compromise between both responses[26].

3. Results and Discussion

3.1 pH_{zpc} determination

A plot of ΔpH as a function of pH_0, resulted in a pH_{zpc} 8.6, see **Figure S1**. An increase in the pH_{ZPC} of CIN (8.6) compared to chitosan (6.3)[15] can be explained by the presence of iron oxides/hydroxides, which give a higher positive charge density on its surface[27]. At pH 4.5, CIN has a positive surface charge, which favors As(V) sorption, because it is present predominantly as $H_2AsO_4^-$ see **Figure S2**[28]. Under these conditions, As(V) could form the ferric arsenate species according to the following reaction[29]:

$$Fe(OH)_2^+ + H_2AsO_4^- = FeAsO_4 + 2H_2O$$

The formation of this specie explains that, in addition to physical sorption, chemical sorption can also take place.

3.2. Effect of pH and iron content

Figure 1 showed a maximum As(V) removal obtained at pH 4.5 (83% removal).

Insert Figure 1 here

At this pH there is a favorable electrostatic attraction between As(V) and CIN, allowing efficient removal of arsenate ions. **Table II** details the batch experiment results, carried out with solutions of As(V) and: a) CIN, b) iron nanoaggregates, and c) chitosan. It can be seen that the CIN material has a higher retention capacity of As(V). Chitosan stabilize the iron nanoparticles preventing their agglutination in the sorption experiments and, in this way, exposing a major surface area per mass unit. The more surface area exposed implies more binding sites available and a higher retention capacity.

Insert Table II here

Elution profiles of columns filled with chitosan and CIN are compared in **Figure 2**. It was evidenced that in the case of removal of As(V) with CIN, As(V) is not detected in the effluent during the first 180 minutes. Therefore, the t_b and the volume of purified water (Vol) increase considerably compared to the unmodified chitosan sorbent.

Insert Figure 2 here

3.3 FTIR, XRD and TGA characterization

In the spectra shown below (**Figure 3**), the characteristic signals of chitosan and CIN after being exposed to arsenate ions are observed.

Insert Figure 3 here

Spectra showed signals between 3500 - 3400 cm^{-1} corresponding to the OH and NH groups vibration, a signal around 2900 cm^{-1} attributed to the CH_2 vibration. Between 1660 and 1652 cm^{-1}, the band was observed due to the C=O bond in the amide group (CO-NH-R, amide band I), while the signal between 1590 - 1550 cm^{-1} is due to the amine group NH-R (amide II). At 1416 cm^{-1}, a band corresponding to the vibration of the OH groups is displayed. The signals in the 1150 - 1070 cm^{-1} range matches to the glycoside bond -C-O-C. The Fe-O bond was observed in the range 560 - 540 cm^{-1}, justifying in this way, the presence of iron oxides. The arsenate group has an absorption band due to the As-O bond located between 610 - 500 cm^{-1}. This band appears with greater intensity in the CIN spectra after being exposed to arsenate ions.

Figure S3 shows the diffractograms of CIN and CIN-As. In the CIN sorbent diffractogram, a characteristic chitosan peak was observed at approximately $2\theta = 20°$. The peaks at 2θ = 30.1, 35.5, 43.1, 71.1, 74.1 can be attributed to (220), (311), (400), (620) and (533) planes respectively of Fe_3O_4 (ICDD 01-075-0033). On the other hand, the peak at 2θ = 40.5 can be assigned to the (101) plane of FeOOH (ICDD 01-076-0123). Additional peaks at 53.7 and 62.7 can be assigned both to (422), (440) planes of Fe_3O_4, and (012), (110) planes of FeOOH. Although Fe(0) could be present, its peak of

greater intensity around 2θ = 42.9 (ICDD03-065-4150) could be overlapped with peak 43.1 attributed to Fe_3O_4. In the CIN-As diffractogram, a marked decrease in the intensity of the peaks mentioned above is observed, so it can be affirmed that the sorption of arsenate ions breaks the semi-crystallinity state of the polymeric portion of the material and iron oxides present in it. Similar results were observed by Wang and colleagues[30].

TGA analysis of CIN and CIN-As was performed to improve the system's chemical-physical characterization (**Figure S4**). Total Fe content found in CIN was 5.8%, by ICP-MS and 4.8% by EDS (see next section). The CIN thermogram showed a water loss of 4.4% in the range of 100 - 200 °C and a mass loss of 78.2% due to the decomposition of the polymer in two stages (range 200 - 550 °C). The CIN-As thermogram showed different behavior. Water loss was less (2.5%) and occurs in the range of 100 - 200 °C. However, no mass loss was observed between 200 and 240 °C. The TGA results obtained were different from those of the pure chitosan polymer reported in the literature[31]. This additional stability to chitosan may be the result of an increase in chitosan stability given by Fe nanoaggregates. CIN decomposition is similar (80% mass loss, range 240 - 530 °C) to the results observed for different oxides of Fe from nanoaggregates. Final residue is a mixture of Fe oxides. The final residue for the CIN-As system is somewhat more significant (11.3%), due to a mixture of Fe and As oxides.

3.4 SEM and EDS

SEM analysis showed homogeneity of size (average 18 µm) and morphology (spherical) of CIN, **Figure 4**. A close up of an individual agglomerate allowed the determination of average particle size, which was 58 nm.

Insert Figure 4 here

EDS spectrum of the composition of nanoparticles showed traces of sodium and sulfur, both due to the chemical synthesis from iron sulfate in alkaline medium (data not shown).

Taking into account the results presented in the previous sections, it is possible to propose that the increased uptake in the hybrid material for As(V) is due to electrostatic interaction and formation of Fe-As compounds on the iron nanoaggregates Surface, as can be seen in **Scheme I**.

Insert scheme I here

3.5 Improvement of the contaminant sorption process in fixed bed columns

Values for each factor generated by the CCD and the responses obtained are shown in **Table III**.

Insert Table III here

An acceptable t_b indicates the column effluent must have an As(V) concentration of 0.05 mg L^{-1} according to the Argentine drinking water standards[12]. Both responses (t_b and Vol) were optimized, generating the desirability function. The results of these analyses are detailed below.

3.6. tb improvement

ANOVA analysis for this model is shown in **Table S2**. Analysis of variance for this response indicates the quadratic model result significant. The lack of adjustment is not significant and indicates that the model has a good correlation with the experimental values. Statistical parameters of the model prediction are shown in **Table S3**. The R^2-predicted and R^2-adjusted values did not show a significant difference, discarding a possible effect of blocking and the presence of outliers, as shown in **Figure S5**. Adequate precision is related to the signal-to-noise ratio, and values greater than 4.0 are considered correct.

As was mentioned before, response t_b can be expressed with a quadratic model using the following mathematical coded expression, **Eq. 4**

$$t_b = 113.69 + 16.53\ H^2 + 93.77\ Q^2 + 93.03\ H - 160.46\ Q - 44.66\ H\ Q \quad \textbf{Eq. 4}$$

The response Surface obtained, **Figure S6**, showed that t_b increase when H increases and decrease when Q increases. This is coherent because: a) an increment in H implies an increment in sorbent mass and thus the number of active sorbent sites increase, resulting in a greater As(V) uptake and b) an increase in Q means that a greater amount

of As(V) is entering the column in less time, which causes saturation of the active sorption sites.

3.7. Vol improvement

The quadratic model for Vol response was significant (**Table S4**) Values of R^2-predicted and R^2-adjusted did not show significant differences (**Table S5**), discarding block effects, and the presence of outliers, **Figure S7**. The signal-to-noise ratio (adequate accuracy), is greater than 4. The lack of adjustment is not significant, indicating the model has a good correlation with experimental values.

Using the coded coefficients, the quadratic model can be expressed by **Eq. 5**

$$Vol = 645.18 + 93.71\ H^2 - 164.67\ Q^2 + 513.77\ H + 42.40\ Q \qquad \textbf{Eq. 5}$$

The graph of the response surface, **Figure S8**, showed that increasing H increases the Vol of purified water due to a more significant number of active sites of the sorbent and therefore the amount of As(V) retained will be higher. From **Figure S8** it can be seen that, at low H, an increment in Q results in a better response for Vol until a maximum Q value, for which Vol response begins to decrease. The same explanation can be raised to high H.

3.8 Desirability Function

When a simple response is being analyzed, the model analysis indicates areas in the design region where the system is likely to give desirable results. However, when

several responses are needed to be simultaneously optimized, the desirability function can be employed, which is a function of more than one response. The desirability function includes the priorities of researchers and desires in building the optimization procedure. The procedure involves creating a function for each individual response (d_i) and finally obtaining a global function D that should be maximized by choosing the best conditions of the designed variables. The function D ranges from 0 (value totally undesirable) to 1 (all responses are in a desirable range simultaneously) and is defined by **Eq. (6),** where d_1, d_2, . . ., d_N correspond to the individual desirability function for each response being optimized:

$$D = [\prod_{n=1}^{N} dn]^{1/N} \qquad \textbf{Eq. 6}$$

Two responses were simultaneously optimized: minimizes tb and maximizes Vol are desirable. After the optimization procedure was carried out a response surface for the global desirability function was built as a function of the influencing factors *H* and *Q*.

The objective was to minimizes the t_b and maximizes the Vol at the same time to reduce operating costs. **Figure 5** shows the response surface for the desirability function. It was found that desirability increases as Q and H increases. As Q increases, the contaminant load on the sorbent is higher, and it saturates more rapidly. However, if the H of the column is increased at the same time, there is a greater amount of sorbent, which would make it possible to obtain a greater quantity of purified water. This compensation effect achieves maximum value for Q = 8.60 mL min^{-1} and H = 2.22 cm with desirability of

0.913. Using the generated desirability function a t_b value of 58.7 min and a volume of purified water of 498.9 mL were predicted.

Insert Figure 5 here

The breakthrough curve for this experimental condition and the adjustment to experimental data made by Thomas[32], Yoon Nelson[33], and Dose-Response[34] models are shown in **Figure S9** and **Table S6**. As can be seen clearly, the Dose-Response model fits the experimental data better than Thomas and Yoon Nelson models.

Experimental value of t_b (58 min) and Vol (490 mL) were obtained. These values are in agreement with those predicted by the desirability function. Thus, it can be said that the desirability function validates the objective of optimizing both responses studied satisfactorily.

Adsorbent reusability was checked by conducting three adsorption‑desorption cycles. The breakthrough time (tb) was 58 min and the volume of water treated (Vb) at breakthrough was 0.49 L in the first cycle.

Desorption/recovery of As(V) from the column was performed with 0.1 M NaOH solution. It was observed that the percentage (%) of As(V) desorption was 95% in the first cycle. The volume of desorption solution employed was 0.05L. Breakthrough time (tb) decreased to 55 min in the second cycle (over 5 % loss of removal capacity). The percentage (%) of As(V) desorption was 75% in the second cycle and breakthrough time (tb) decreased to 35 min in the second cycle (over 40 % loss of removal capacity).

Loss of removal capacity was probably due to As(V) kept bonded to CIN blocking active sites and/or partial modification of CIN surface structure by NaOH solution modifying the sorption properties of the material. The effluent water quality suggests that the As(V) removed water by CIN could be used for household purposes.

4. Conclusions

Continuous sorption of As(V) in groundwater was studied using a hybrid material as sorbent: CIN. SEM, EDS, TGA, XRD and FTIR spectroscopic techniques were applied to characterize the sorbent. The results observed in FTIR and XRD evidenced the presence of the main components of the material: chitosan and iron (such as oxides, hydroxides, and probably zero-valent iron). FTIR spectra of As and the decrease in the degree of crystallinity by XRD confirm As(V) sorption. Batch studies showed synergy of the material for the sorption of As(V). The use of the experimental design in fixed bed column studies was successfully applied. It allowed an integral study of the column sorption process. Having a multi-response model allowed the generation of the desirability function by optimizing the process for the two responses studied: tb and Vol.

Acknowledgments

Authors acknowledge the contribution of Dr. Agustin Frattini for carried out the TGA measurements; National Agency of Scientific and Technological Promotion (ANPCyT) PICT 2016-1611, Santa Fe Province Agency of Science, Technology and Innovation

ASACTEI N° AC 2015-0005 and National University of Rosario (UNR) BIO517 for financial support.

References

1. Litter M, La problemática del arsénico en la Argentina: el HACER. Rev. Soc. Argent. Endocrinol. Ginecol. Reprod. (SAEGRE) 17(2): 5- 10 (2015).

2. Murcott S. Arsenic Contamination in the World, An International Sourcebook. IWA Publishing, London. National Research Council (US), Subcommittee on Arsenic in Drinking Water; 2012.

3. Sodhi K, Kumar M, Agrawal P, Singh D. Perspectives on arsenic toxicity, carcinogenicity and its systemic remediation strategies. Environ. Technol. & Innov. 16: 1- 16 (2019).

4. Jang Y, Somanna Y, Kim H. Source, distribution, toxicity and remediation of arsenic in the environment – a review. IJAES 11: 559- 581 (2016).

5. Carlin D, Naujokas M, Bradham K, Cowden J, Heacock M, Henry H, Lee J, Thomas D, Thompson C, Tokar E, Waalkes M, Birnbaum L, Wa W. Arsenic and environmental health: state of the science and future research opportunities. Environ. Health Perspect. 124(7): 890- 899 (2016).

6. Shankar S, Shanker U, Shikha S, Arsenic contamination of groundwater: a review of sources, prevalence, health risks, and strategies for mitigation. Scientific World Journal. 1-18 (2014).

7. Mariño E, Ávila G, Bhattacharya P, Schulz C. The occurrence of arsenic and other trace elements in groundwaters of the southwestern Chaco-Pampean plain, Argentina. J. South American Earth Sci. 100: 1- 7 (2020).

8. Nicolli H, Bundschuh J, Blanco M, Tujchneider O, Panarello H, Dapeña C, Rusansky J. Arsenic and associated trace-elements in groundwater from the Chaco-Pampean plain, Argentina: results from 100 years of research. Sci. Total Environ. 429: 36- 56 (2012).

9. Argos M, Kalra T, Pierce B, Chen Y, Parvez F, Islam T, Ahmed A, Hasan R, Hasan K, Sarwar G, Levy D, Slavkovich V, Graziano J, Rathouz P, Ahsan H. A Prospective Study of Arsenic Exposure From Drinking Water and Incidence of Skin Lesions in Bangladesh. Am. J. Epidemiol. 174(2): 185- 194 (2011).

10. Bardach A, Ciapponi A, Soto N, Chaparro M, Calderon M, Briatore A, Cadoppi N, Tassara R, Litter M. Epidemiology of chronic disease related to arsenic in Argentina: A systematic review, Science of the Total Environment. 538: 802-816 (2015).

11. World Health Organization (WOH), Guidelines for drinking- water quality. Fourth edition. pp. 631 (2017).

12. Código Alimentario Argentino (CAA), 2019. Capítulo XII. Art. 982 Al 1079 - Bebidas Hídricas, Agua Y Agua Gasificadas. http://www.anmat.gov. ar/alimentos/codigoa/CAPITULO_XII.pdf (accessed november 9, 2019).

13. Litter M, Ingallinella A, Olmos V, Savio M, Botto L, Farfán Torres E, Taylor S, Frangie S, Difeo G, Herkovits J, Schalamuk I, González M, Berardozzi E, García Einschlag F, Bhattacharya P, Ahmad A. Arsenic in Argentina: Technologies for arsenic

removal from groundwater sources, investment costs and waste management practices. Science of the Total Environment. 690: 778-789 (2019).

14. Bertoni F, Medeot A, González J, Sala L, Bellú S. Application of green seaweed biomass for MoVI sorption from contaminated waters. Kinetic, thermodynamic and continuous sorption studies. Journal of Colloid and Interface Science. 446: 122-132 (2015).

15. Bertoni F, González J, García S, Sala L, Bellú S. Application of chitosan in removal of molybdate ions from contaminated water and groundwater. Carbohydr. Polym. 180: 55-62 (2018).

16. Pérez Mora B, Bellú S, Mangiameli M, García S, González J. Optimization of continuous arsenic biosorption present in natural contaminated groundwater. J. Chem. Technol. Biotechnol. 94: 547-555 (2019).

17. Blanes P, Bordoni M, González J, García S, Atria A, Sala L, Bellú S. Application of soy hull biomass in removal of Cr (VI) from contaminated waters. Kinetic, thermodynamic and continuous sorption studies. J Environ. Chem. Engin. 4: 516-526 (2016).

18. Shakoor M, Niazi N, Bibi I, Shahid M, Saqib Z, Nawaz M, Shaheen S, Wang H, Tsang D, Bundschuh J, Ok Y, Rinklebe J. Exploring the arsenic removal potential of various biosorbents from water. Environ. Int. 123: 567-579 (2019).

19. Pérez Mora B, Bellú S, Mangiameli M, González J. Response surface methodology and optimization of arsenic continuous sorption process from contaminated water using chitosan. Journal of Water Process Engineering. 32: 100913-100922 (2019).

20. Arcibar-Orozco J, Delgado-Balbuena J, Rios-Hurtado J, Rangel-Mendez J. Influence of iron content, surface area and charge distribution in the arsenic removal by activated carbons. Chemical Engineering Journal 249: 201-209 (2014).

21. Aredes S, Klein B, Pawlik M. The removal of arsenic from water using natural iron oxide minerals. Journal of Cleaner Production 29-30: 208-213 (2012).

22. Cortina J, Fiúza A, Silva A, Litter M. In-situ technologies for groundwater treatment: the case of arsenic. Renewable energy applications for freshwater production. CRC/Balkema Editor. London; pp. 35 – 45 (2014).

23. Thomas H. Heterogeneous ion exchange in a flowing system. J. Am, Chem. Soc. 66: 1664-1666 (1944).

24. Yoon Y, Nelson J. Application of gas adsorption kinetics theoretical model for respirator cartridge service life. Am. Ind. Hyg. Assoc. J. 45: 509-516 (1984).

25. Yan G, Viraraghavan T, Chen M. Heavy metal removal in a biosorption column by immobilized M. Rouxii biomass. Adsorp. Sci. Technol. 19: 25-43 (2001).

26. Anderson M, Whitcomb P. RSM Simplified optimizing processes using response surface methods for design of experiments; 2º Ed; CRC Press Taylor & Francis Group 2016.

27. Cornell R. The Iron oxides; 2º Ed; Wiley-VCH 2003.

28. Wulfsberg G. Inorganic Chemistry, University Science Books, United States, 2000.

29. Mamindy-Pajany Y, Hurel C, Marmier N, Roméo M. Arsenic(V) adsorption from aqueous solution onto goethite, hematite, magnetite and zero-valent iron: Effects of pH, concentration and reversibility. Desalination. 281: 93-99 (2011).

30. Wang X, Du Y, Fan L, Liu H, Hu Y. Chitosan- metal complexes as antimicrobial agent: synthesis, characterization and Structure-activity study. Polym. Bull. Berl. 55: 105-113 (2005).

31. Abdou E, Nagy K, Elsabee M. Extraction and characterization of chitin and chitosan from local sources. Biores. Technol. 99: 1359-1367 (2008).

32. Thomas H. Heterogeneous Ion Exchange in a Flowing System. J. Am. Chem. Soc. 66: 1664-1666 (1944).

33. Yoon Y, Nelson J. Application of gas adsorption kinetics I. A theoretical model for respirator cartridge service life, Am. Ind. Hyg. Assoc. J. 45: 509-516 (1984).

34. Yan G, Viraraghava, T, Chen M. A new model for heavy metal removal in a biosorption column. Adsorption Science & Technology, 19: 25-43 (2001).

Figure 1

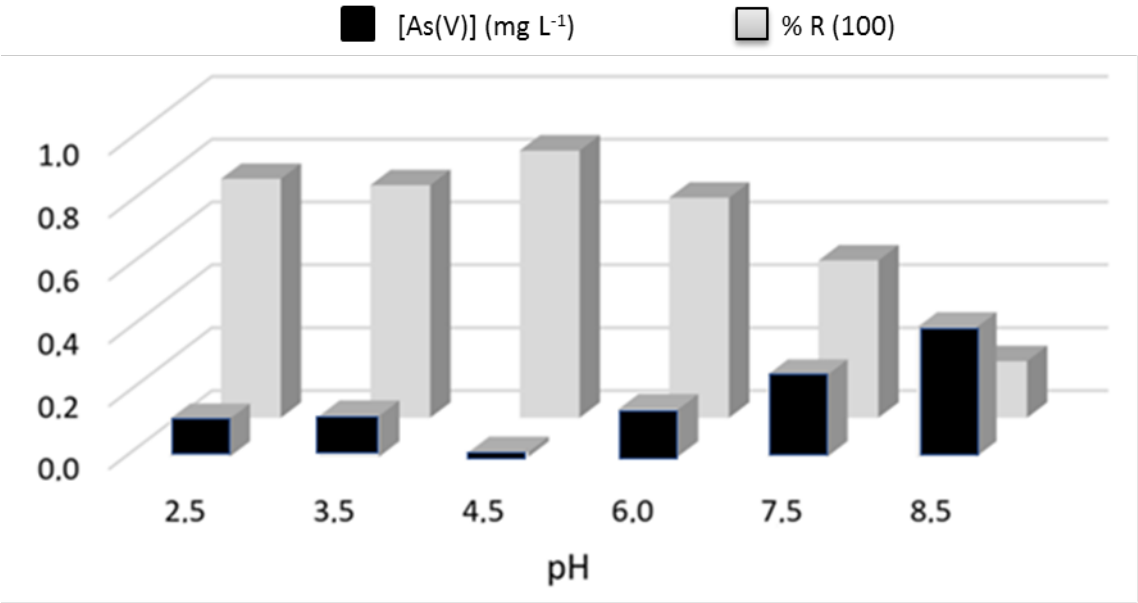

Figure 2

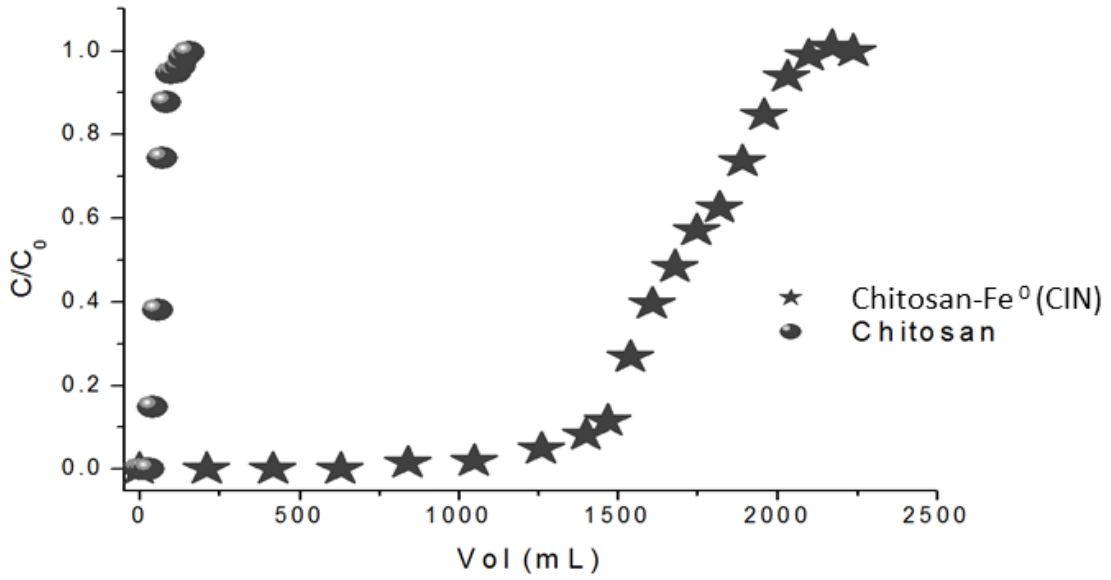

Figure 3

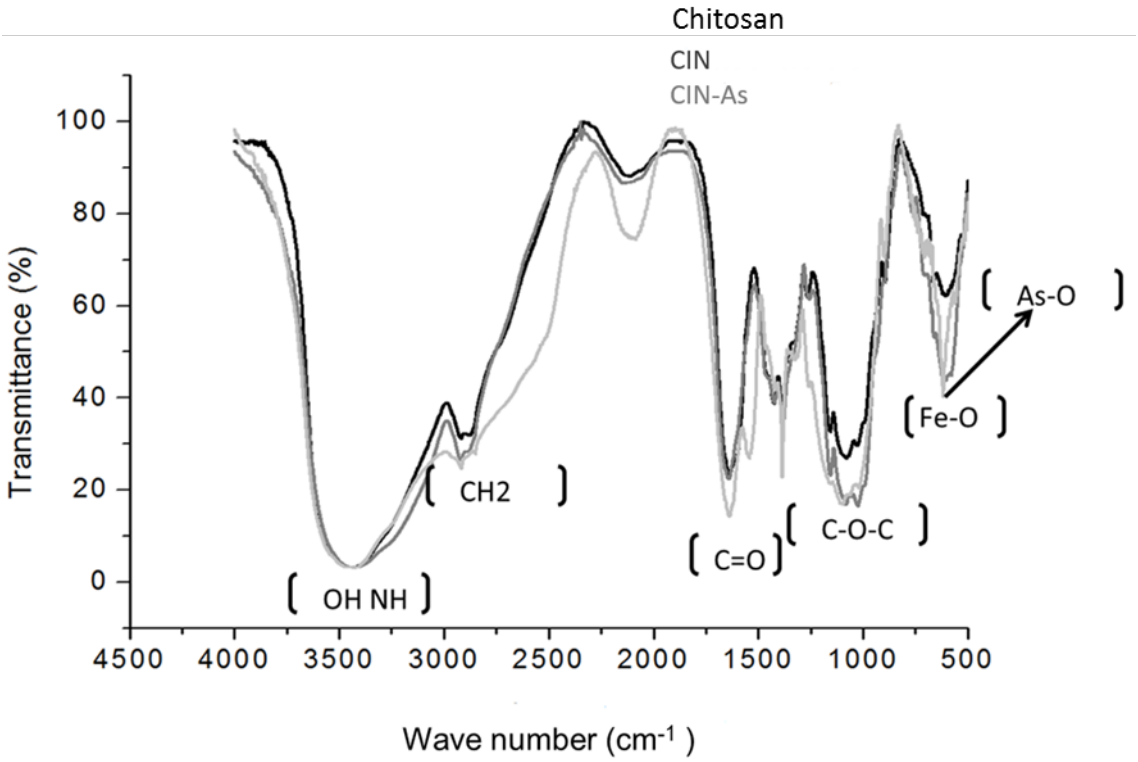

Figure 4

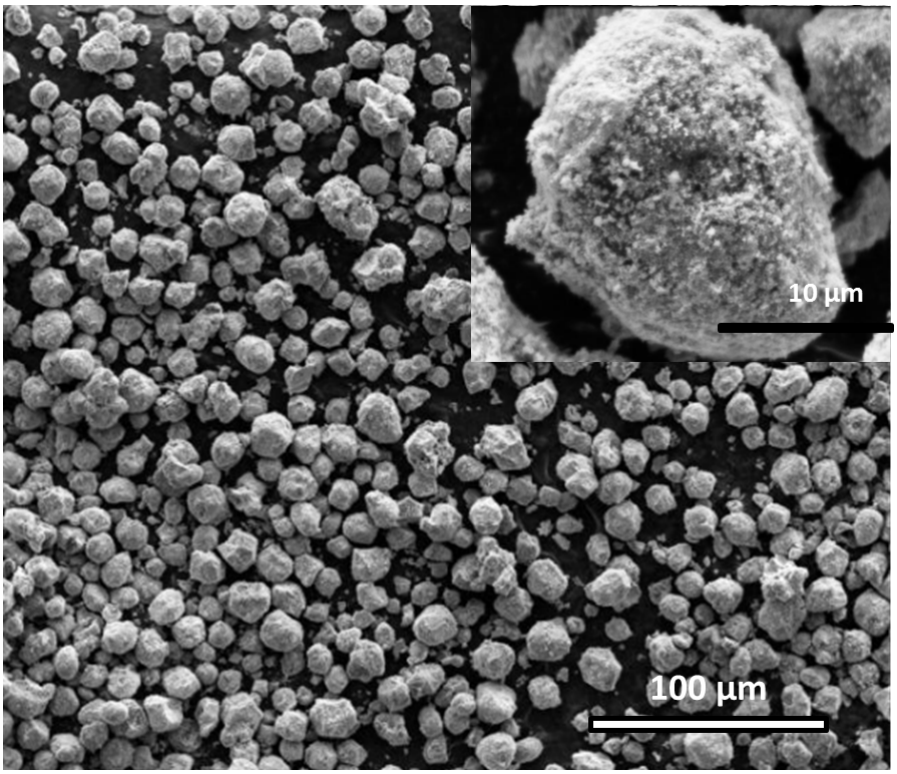

Figure 5

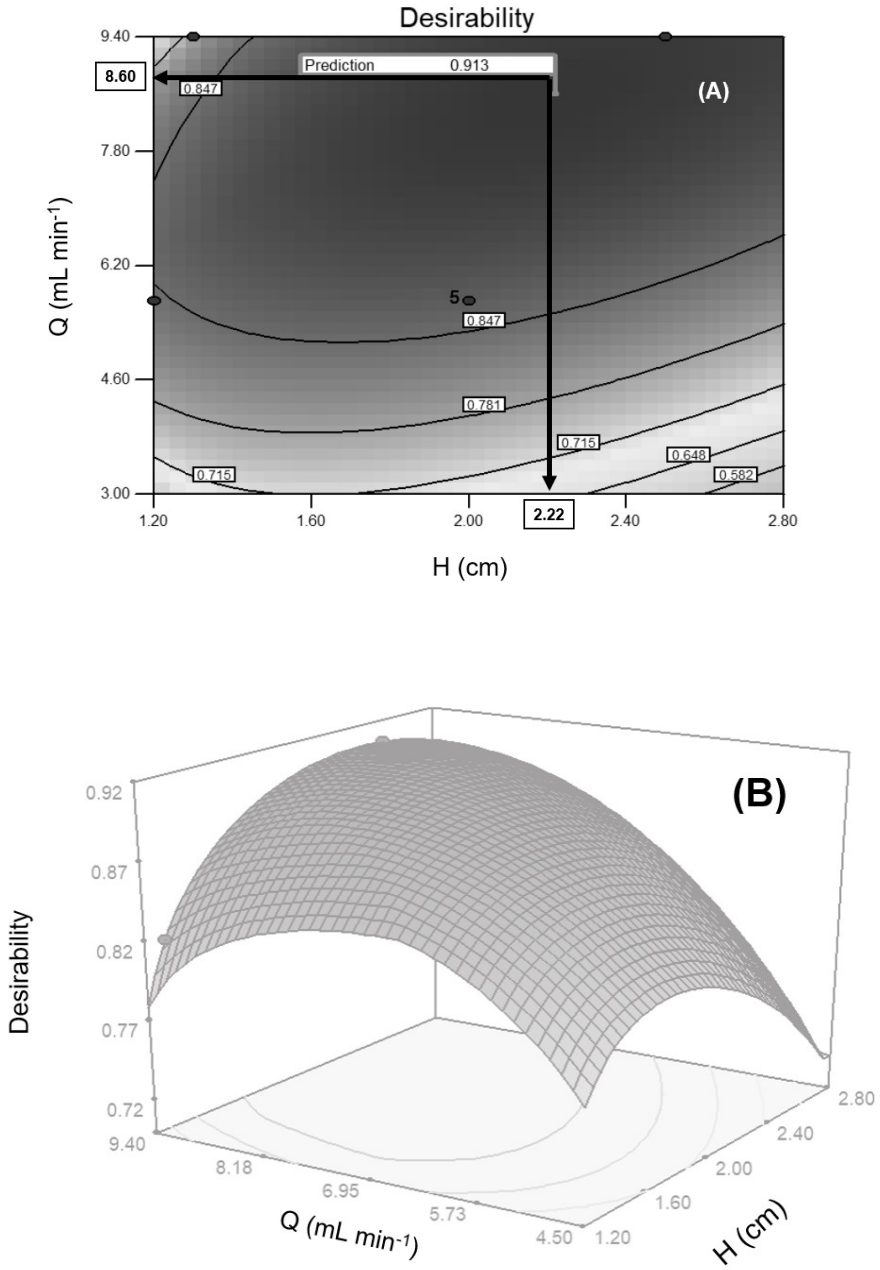

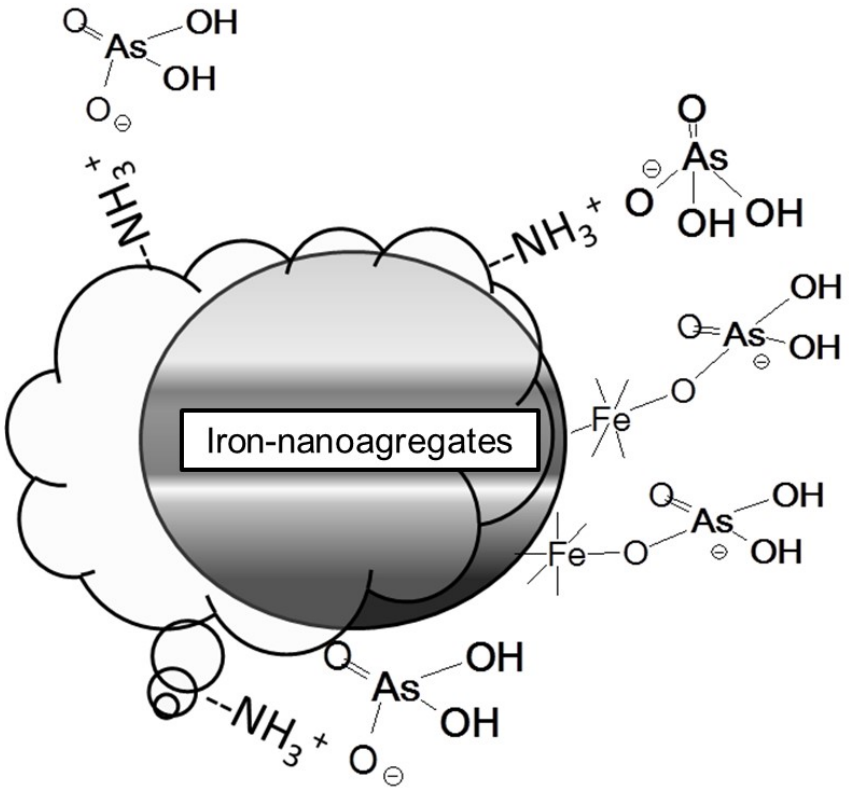

Scheme 1. Arsenate (As(V)) sorption mechanism on CIN.

Table I. Coded levels for independent factors used in the experimental design.

Factors	Symbol	Coded levels				
		$-\alpha$	-1	0	1	$+\alpha$
H (cm)	X_1	0.90	1.20	2.00	2.80	3.10
Q (mL min^{-1})	X_2	0.50	2.00	5.70	9.40	10.00

Table II. As(V) removal.[b]

Material	Mass (g)	As(V) remaining (mg L^{-1})	As(V) removal (%)
chitosan	3.99	15.60	20.30
iron nanoaggregates	0.20	9.81	53.13
CIN	4.20	0.51	97.50

[b]Reaction conditions: $[As(V)]_0$ = 20 mg L^{-1}, pH = 4.5; T = 25°C, V_f = 200 mL.

Table III. Values for each factor generated by the CCD and the responses obtained.

Column	H (cm)	Q (mL min^{-1})	t_b (min)	Vol (mL)
1	1.20	5.70	33	188.1
2	2.80	2.00	522	1044.0
3	0.90	5.70	18	102.6
4	2.00	5.70	110	627.0
5	2.50	9.40	90	846.0
6	3.10	5.70	271	1544.7
7	2.00	0.50	525	262.5
8	2.00	5.70	125	712.5
9	2.00	5.70	118	672.6
10	1.20	9.40	22	206.8
11	2.00	10.00	45	450.5
12	2.00	5.70	109	621.3
13	2.00	5.70	109	621.3